



ACADEMIC  
PRESS

Available online at [www.sciencedirect.com](http://www.sciencedirect.com)

SCIENCE @ DIRECT®

Journal of Solid State Chemistry 173 (2003) 251–258

JOURNAL OF  
SOLID STATE  
CHEMISTRY

<http://elsevier.com/locate/jssc>

# Lithium monosilicide (LiSi), a low-dimensional silicon-based material prepared by high pressure synthesis: NMR and vibrational spectroscopy and electrical properties characterization

Linda A. Stearns,<sup>a</sup> Jan Gryko,<sup>b</sup> Jason Diefenbacher,<sup>c</sup> Ganesh K. Ramachandran,<sup>d</sup> and Paul F. McMillan<sup>e,f,\*</sup>

<sup>a</sup> Department of Chemical & Materials Engineering, Arizona State University, Tempe, AZ 85287, USA

<sup>b</sup> Department of Physical & Earth Sciences, Jacksonville State University, Jacksonville, AL 36265, USA

<sup>c</sup> Center for Solid State Science, Arizona State University, Tempe, AZ 85287, USA

<sup>d</sup> Department of Physics & Astronomy, Arizona State University, Tempe AZ 85287, USA

<sup>e</sup> Davy Faraday Research Laboratories at the Royal Institution of Great Britain, London W1S 4BS, UK

<sup>f</sup> Christopher Ingold Laboratory, Department of Chemistry, University College London, London WC1H 0AJ, UK

Received 21 August 2002; received in revised form 17 December 2002; accepted 18 December 2002

## Abstract

Lithium monosilicide (LiSi) was formed at high pressures and high temperatures (1.0–2.5 GPa and 500–700°C) in a piston-cylinder apparatus. This compound was previously shown to have an unusual structure based on 3-fold coordinated silicon atoms arranged into interpenetrating sheets. In the present investigation, lowered synthesis pressures permitted recovery of large (150–200 mg) quantities of sample for structural studies via NMR spectroscopy (<sup>29</sup>Si and <sup>7</sup>Li), Raman spectroscopy and electrical conductivity measurements. The <sup>29</sup>Si chemical shift occurs at –106.5 ppm, intermediate between SiH<sub>4</sub> and Si(Si(CH<sub>3</sub>)<sub>3</sub>)<sub>4</sub>, but lies off the trend established by the other alkali monosilicides (NaSi, KSi, RbSi, CsSi), that contain isolated Si<sub>4</sub><sup>4–</sup> anions. Raman spectra show a strong peak at 508 cm<sup>–1</sup> due to symmetric Si–Si stretching vibrations, at lower frequency than for tetrahedrally coordinated Si frameworks, due to the longer Si–Si bonds in the 3-coordinated silicide. Higher frequency vibrations occur due to asymmetric stretching. Electrical conductivity measurements indicate LiSi is a narrow-gap semiconductor ( $E_b \sim 0.057$  eV). There is a rapid increase in conductivity above  $T = 450$  K, that might be due to the onset of Li<sup>+</sup> mobility.

© 2003 Elsevier Science (USA). All rights reserved.

**Keywords:** Lithium monosilicide; Silicides; High pressure synthesis; Low-dimensional silicon; Solid-state NMR; Raman scattering; Metastable phase transitions

## 1. Introduction

Silicon is usually found in tetrahedral coordination in solid state and molecular compounds. However, the polyanionic compounds known as “Zintl phases” often contain silicon in unusual coordination states, including three-coordinated environments [1–3]. It is important to characterize the electronic properties and local structural environment of silicon in these novel low-dimensional Si-based materials. Zintl phases are formed between

electropositive elements and Ga, As, Al, Sn, Si, Ge, etc. According to the Zintl–Klemm concept, developed to account for the unusual bonding in these compounds, the average coordination of the more electronegative element is determined by an  $8 - N$  rule, where  $N$  is the number of valence electrons per anion [1–3]. In the alkali monosilicide Zintl phases ( $MSi$ ), there are formally five valence electrons per silicon anion and, therefore, each silicon atom forms  $8 - 5 = 3$  bonds with its Si neighbours. In NaSi and the heavier alkali monosilicides ( $M = K, Rb, Cs$ ), the 3-coordinated bonding is expressed by formation of isolated  $[Si_4]^{4-}$  tetrahedra, that are isostructural with the P<sub>4</sub> units in elemental white phosphorus (Si<sup>–</sup> and P are isoelectronic species). Electroneutrality is then achieved by surrounding each

\*Corresponding author. Christopher Ingold Laboratory, Department of Chemistry, University College London, London WC1H 0AJ, UK.

E-mail address: [p.f.mcmillan@ucl.ac.uk](mailto:p.f.mcmillan@ucl.ac.uk) (P.F. McMillan).

$[\text{Si}_4]^{4-}$  group with four  $\text{Na}^+$  ions (Fig. 1). However, the structure of LiSi is different.

The Zintl phase chemistry of Li-containing compounds has received special attention because of the wide range of structures formed [3]. However, despite extensive studies, lithium monosilicide (LiSi) long remained a “missing” member of the alkali silicide series [3–5]. All of the other alkali monosilicides had been described previously, and several binary compounds were already known in the Li–Si system ( $\text{Li}_{22}\text{Si}_5$ ,  $\text{Li}_{13}\text{Si}_4$ ,  $\text{Li}_7\text{Si}_3$ ,  $\text{Li}_{12}\text{Si}_7$ ) [3,6]. However, repeated attempts to synthesize LiSi had yielded only mixtures of elemental Si and other  $\text{Li}_x\text{Si}_y$  phases. Evers et al. [4] recently analysed the problem, and demonstrated that the “synthesis barrier” to LiSi was due to kinetic

factors, rather than to any intrinsic instability of the monosilicide phase. These researchers showed that LiSi is unstable to decomposition into  $\text{Li}_{12}\text{Si}_7 + \text{Si}$  at  $T > 470^\circ\text{C}$ : i.e., the reverse of the formation reaction (1):



At temperatures lower than this value, formation of LiSi is hampered by crystallization kinetics, and other phase mixtures (e.g.,  $\text{Li}_{12}\text{Si}_7 + \text{Si}$ ) are obtained metastably instead. Evers et al. then recognized that the formation of LiSi either by reaction (1) or directly from the elements (reaction (2)):

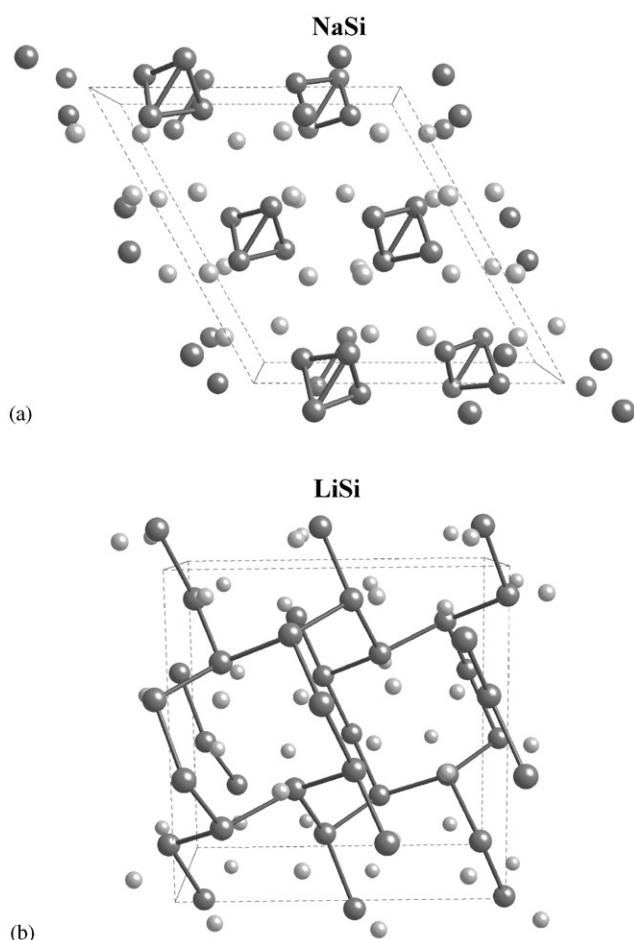


Fig. 1. (a) Crystal structure for NaSi (monoclinic  $C2/c$  structure).  $[\text{Si}_4]^{4-}$  ions form isolated tetrahedra, analogous to  $\text{P}_4$  groups in white phosphorous, about which  $\text{Na}^+$  ions (grey spheres) are arranged. View along  $\sim[010]$ . (b) Crystal structure for LiSi, illustrating three-fold coordinated  $\text{Si}^-$  ions forming interconnected chains and pucker eight-membered rings (isostructural with the high-pressure form of black phosphorus). Cavities in the  $(\text{Si}^-)_n$  framework of LiSi are occupied by  $\text{Li}^+$  ions (grey spheres), forming approximately tetrahedral groupings of 4  $\text{Li}^+$  ions, isolated from each other by the  $(\text{Si}^-)_n$  backbone. View along  $\sim[001]$ .

was associated with a negative  $\Delta V_{\text{formation}}$ , indicating increased thermal stability for the monosilicide at high pressure. They used this observation to carry out the first successful syntheses of LiSi at high  $P$ – $T$  conditions (4 GPa;  $600^\circ\text{C}$ ), followed by recovery of the monosilicide to ambient conditions, and determination of its crystal structure [4,5]. Thermal analysis on recovered material was used to demonstrate that the compound was stable to  $470^\circ\text{C}$ , where it decomposed into  $\text{Li}_{12}\text{Si}_7 + \text{Si}$  (Fig. 2).

X-ray determination of the new compound revealed that LiSi was not isostructural with the other alkali monosilicides, but that it contained a 3-dimensional network of 3-coordinated  $\text{Si}^-$  anions analogous to the structure of black phosphorus [4,5,7] (Fig. 1). This structure was already known for LiGe at ambient  $P$  [8]. The Si–Si bonding pattern forms pucker 8-membered rings that are linked together into interpenetrating sheets, forming cavities 6–8 Å across. Within these cavities in the anionic  $(\text{Si}^-)_n$  framework, the  $\text{Li}^+$  ions form approximately tetrahedral groupings (Fig. 1).

It was of interest to determine the  $^{29}\text{Si}$  NMR spectrum of this new phase with its unusual Si coordination and connectivity, as well as its electrical conductivity as a function of temperature. In order to carry out these measurements, we needed to obtain 100–200 mg quantities of the new phase. To achieve their high  $P$ – $T$  synthesis of LiSi, Evers et al. loaded mixtures of  $\text{Li}_{12}\text{Si}_7 + \text{Si}$  into BN or Mo capsules, and carried out reaction (1) in a belt-type high pressure device [4]. In our work, we have extended LiSi syntheses (via reaction (2)) into a lower pressure regime (1–3 GPa) that is more readily accessible to piston-cylinder apparatus, resulting in preparation of significantly larger amounts of the new compound ( $\sim 150$  mg per run). These syntheses will also provide useful quantities of material for use of LiSi as a precursor for new Si-based clathrates [9–12], as well as for future structural studies and physical properties measurements.

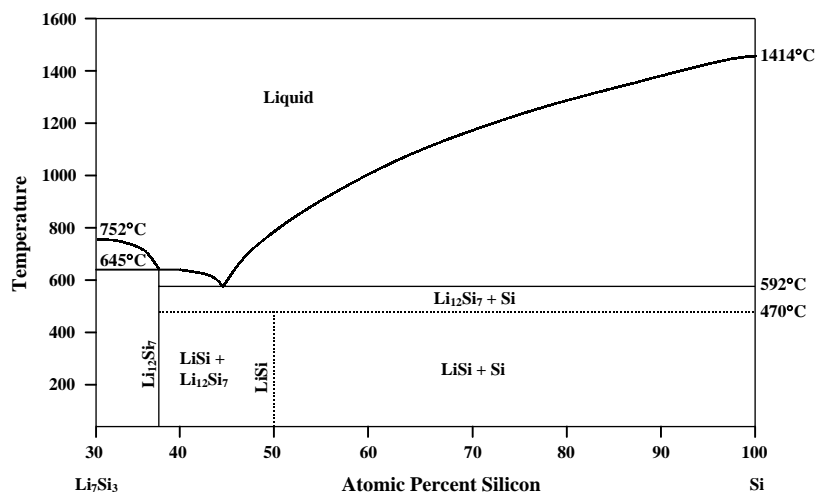


Fig. 2. Schematic binary phase diagram for the Li–Si system at ambient pressure, in the region of stability of the monosilicide LiSi, based on available thermodynamic data (Refs. [2,4]). LiSi decomposes to a mixture of  $\text{Li}_{12}\text{Si}_7$  and Si above 470°C. The decomposition reaction ( $12\text{LiSi} = \text{Li}_{12}\text{Si}_7 + 5\text{Si}$ ) is associated with a positive volume change ( $\Delta V = 13.6\text{ cm}^3$ ), so that the stability field of the monosilicide LiSi increases with applied pressure.

## 2. Experimental

LiSi was obtained in a piston-cylinder apparatus using stainless steel capsules, at  $P = 1\text{--}2.5\text{ GPa}$  and  $T = 500\text{--}700^\circ\text{C}$ . Near-stoichiometric mixtures of Li and Si (usually containing a slight excess of Li) were first heated to  $400^\circ\text{C}$  in a  $\text{ZrO}_2$  crucible.  $\sim 250\text{ mg}$  of the resulting sintered precursor was packed into stainless steel capsules for high  $P$ – $T$  treatment. Run products were analysed via powder X-ray diffraction. The other alkali monosilicides investigated in the study (NaSi, RbSi, CsSi) were prepared by mixing a slight excess of each alkali metal with Si powder and placing the powder in a Ta crucible with a lid, sealed inside a steel vessel, and heating at  $650^\circ\text{C}$  for 20–40 h. All manipulations were carried out in a glove box under inert atmosphere, with  $< 3\text{ ppm O}_2/\text{H}_2\text{O}$ .

Solid state nuclear magnetic resonance (NMR) spectroscopy was carried out using a Varian-Unity spectrometer (9.4 T), corresponding to a Larmor frequency of 155.5 MHz for  $^7\text{Li}$  and 79.5 MHz for  $^{29}\text{Si}$ . Magic angle spinning (MAS) NMR spectra were obtained using Jakobsen 4–5 mm probes, with sintered  $\text{Si}_3\text{N}_4$  rotors spinning at 6–12 kHz. Dry  $\text{N}_2$  was used to drive the rotors to prevent reaction of the silicides with  $\text{O}_2/\text{H}_2\text{O}$  from air. Raman spectra were obtained using  $\text{Ar}^+$  excitation (514.5 nm) and a modified ISA S-3000 system with CCD detector in an airtight cell with  $\text{SiO}_2$  windows. Electrical conductivity measurements were obtained by clamping thin-pressed LiSi pellets between Pt electrodes and sealing the electrode and thermocouple assemblies in an air-tight, stainless-steel probe under high-pressure argon.

## 3. Results and discussion

The results of our piston-cylinder synthesis studies demonstrate that LiSi can be readily synthesized in good yield in the pressure range 1–2.5 GPa, at  $T = 500\text{--}700^\circ\text{C}$  (Fig. 3). Our observations indicated that both kinetic and thermodynamic factors remain important in controlling the monosilicide synthesis at high pressure. In our runs, LiSi always formed the principal product, but  $\text{Li}_{12}\text{Si}_7$  and/or elemental Si were usually also present as minor impurity phases. For example, one synthesis run at 1 GPa and  $500^\circ\text{C}$  (initial ratio 1.3 Li: 1.0 Si; 2 h run time) yielded 17%  $\text{Li}_{12}\text{Si}_7$  and 24% Si and 59% LiSi (estimated from relative X-ray peak intensities) (Fig. 3). For a similar synthesis at 1.75 GPa and  $700^\circ\text{C}$ , the amounts of  $\text{Li}_{12}\text{Si}_7$  and Si among the products dropped to  $\sim 3\%$ . Lengthening run time or increasing synthesis temperature generally increased the amount of Si present in the product, presumably due to loss of volatile Li from the charge. Increasing the amount of Li present in the starting mixture resulted in larger initial amounts of  $\text{Li}_{12}\text{Si}_7$  being formed during the run.  $\text{Li}_{12}\text{Si}_7$  could only be completely eliminated from the products by increasing the run pressure to 2–2.5 GPa, and running at  $600\text{--}700^\circ\text{C}$  for 1–2 h. We found that LiSi could also be obtained at much lower temperatures at high pressure: one run at 2 GPa,  $250^\circ\text{C}$  for 16 h with an initial ratio Li:Si = 1.8:1 resulted in formation of comparable amounts of LiSi,  $\text{Li}_{12}\text{Si}_7$  and Si. Our “best” samples (i.e., with  $\text{Li}_{12}\text{Si}_7/\text{Si}$  impurity content  $< 3\%$ ) were obtained with  $P > 1.75\text{ GPa}$  and  $T = 600\text{--}700^\circ\text{C}$ , with  $\sim 30\%$  excess of Li in the starting material. The sample used for the physical properties

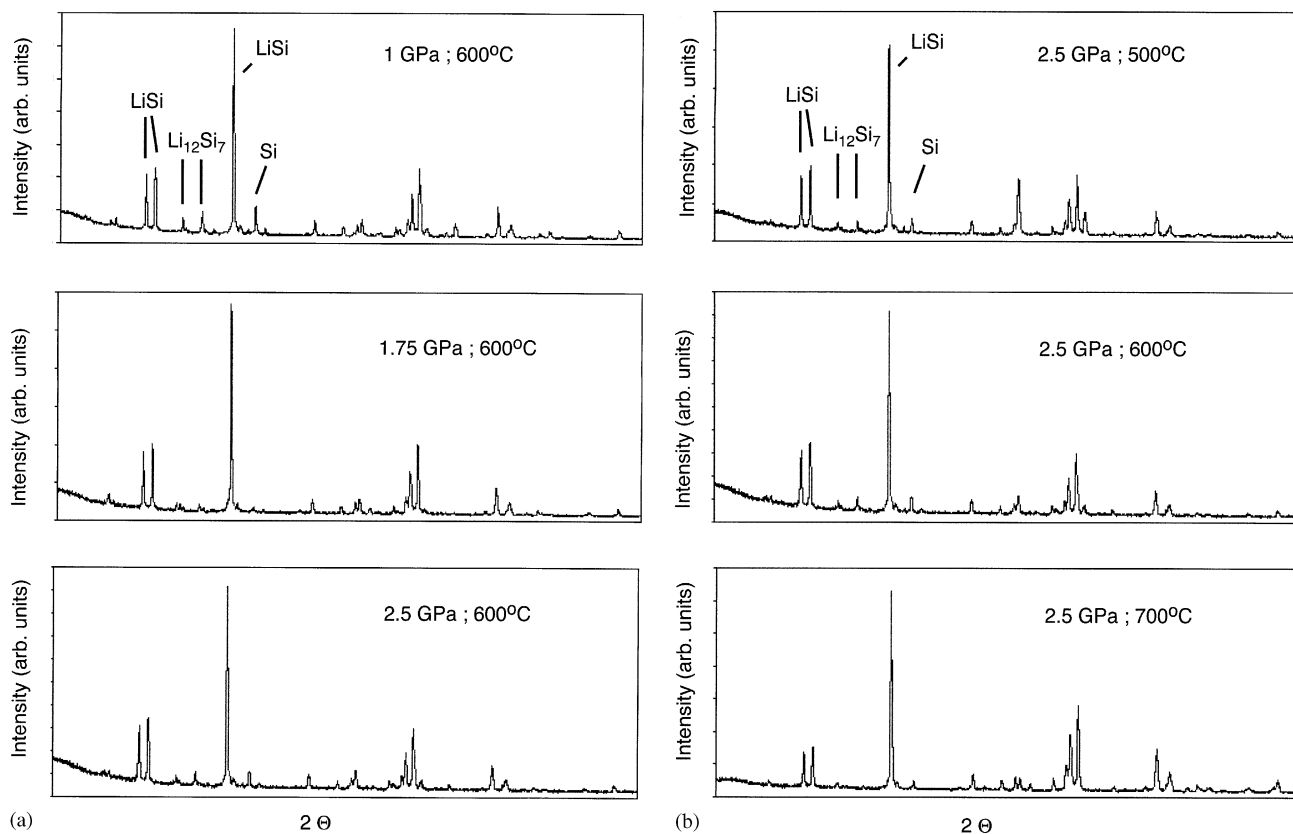


Fig. 3. (a) Representative powder diffraction patterns for LiSi formed from the elements (Si with a slight Li excess) at pressures between 1 and 2.5 GPa (10–25 kbar), at  $T = 600^\circ\text{C}$  (run times = 2 h). The principal product is LiSi for all run pressures. As the synthesis pressure is lowered, impurity phases ( $\text{Li}_{12}\text{Si}_7$  and elemental Si) are generally found in the run products in greater quantity (3–5%). (b) Powder diffraction patterns for LiSi formed from the elements at 2.5 GPa (25 kbar), for temperatures ranging from  $500^\circ\text{C}$  to  $700^\circ\text{C}$ . The “best” synthesis conditions (i.e., lowest quantity of “impurity” phases present) were obtained for  $P = 2.5$  GPa and  $T = 700^\circ\text{C}$ .

studies reported here was prepared at  $P = 2.5$  GPa,  $T = 700^\circ\text{C}$ , with starting ratio 1.3 Li: 1.0 Si, heated at pressure for 2 h run time: the yield was  $\sim 150$  mg in a single run. The powder X-ray pattern is shown in Fig. 4. Structure refinement by the Rietveld method (using the GSAS set of programmes [13]) gave cell parameters and atomic positions that were essentially identical with the previous single crystal study [4] (Table 1).

Our synthesis results permit us to make some observations regarding the thermodynamic basis for the synthesis of LiSi at high pressure. In their pioneering work, Evers et al. noted that the product of reaction (1) was 6% denser than the starting mixture, that then permitted the synthesis at high pressure. Using the recovered monosilicide phase, they measured an endothermic enthalpy for the reverse of reaction (1):  $\Delta H = +0.9 (\pm 0.2)$  kJ/mol. Using these same thermodynamic quantities ( $\Delta V$ ,  $\Delta H$ ), we estimate that the decomposition temperature of LiSi via the reverse of reaction (1) should increase by  $\sim 5$ – $10^\circ$  between ambient  $P$  and 4 GPa. However, Evers et al. obtained the LiSi phase at  $T = 600^\circ\text{C}$  at  $P = 4$  GPa [4]. This lies well above the decomposition temperature suggested by the thermodynamic analysis. We have confirmed this result in our

work: LiSi is readily obtainable from the elements or  $\text{Li}_{12}\text{Si}_7 + \text{Si}$  mixtures at temperatures up to  $700^\circ\text{C}$  (973 K), even for pressures as low as 1 GPa. These observations indicate either that the stability relations of the  $\text{Li}_x\text{Si}_y$  phases in the vicinity of the LiSi compound require further investigation, or that metastable formation of the monosilicide phase becomes kinetically favoured at high pressure.

The Raman spectrum of LiSi is shown in Fig. 5. There is no evidence in the spectrum for elemental Si, which would give rise to a strong peak at  $521\text{ cm}^{-1}$ . The spectrum was obtained using a microbeam Raman instrument: obviously the Si impurity present in the sample formed distinct grains that were not encountered in the experiment. The dominant line for LiSi is an asymmetric band with its maximum at  $508\text{ cm}^{-1}$ , that we assign to symmetric Si–Si stretching vibrations within the pyramidal  $\text{SiSi}_3$  units. The frequency is lowered compared with diamond-structured silicon, consistent with the longer Si–Si bond lengths in LiSi ( $2.417\text{ \AA}$  vs.  $2.352\text{ \AA}$ ). As for elemental Si, second order features occur in the  $800$ – $1100\text{ cm}^{-1}$  region. A new weak band appears at  $622\text{ cm}^{-1}$ , that we assign to asymmetric Si–Si stretching vibrations within the 3-coordinated silicide

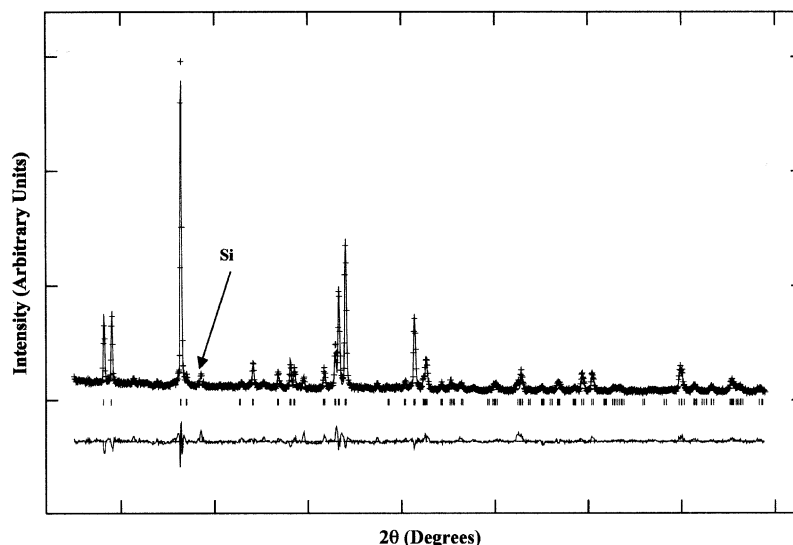


Fig. 4. Result of a Rietveld structure refinement for LiSi synthesized at 25 kbar, 700°C for 2 h. duration. The experimental data are indicated by + marks, and the solid line represents the fit. The positions of reflections calculated by the GSAS program are indicated by tick marks. A small peak due to elemental Si (3%) is indicated by an arrow and was included in the fit. The difference between experimental and fitted profiles is shown below. Refined structural parameters are given in Table 1.

Table 1  
Structure refinement results for LiSi

Atom	<i>x</i>	<i>y</i>	<i>z</i>	<i>U</i> <sub>iso</sub> (Å <sup>2</sup> )
Si	0.0111(4)	0.9522(4)	0.5937(4)	0.025
Li	0.0810(5)	0.8860(5)	0.0602(5)	0.068

Space group *I*4<sub>1</sub>/*a*; *a* = 9.354(3) Å; *c* = 5.746(3) Å; *V* = 502.8 Å<sup>3</sup>  $\chi^2$  = 3.68; Residuals: *R*<sub>p</sub> = 0.068, *R*<sub>wp</sub> = 0.087.

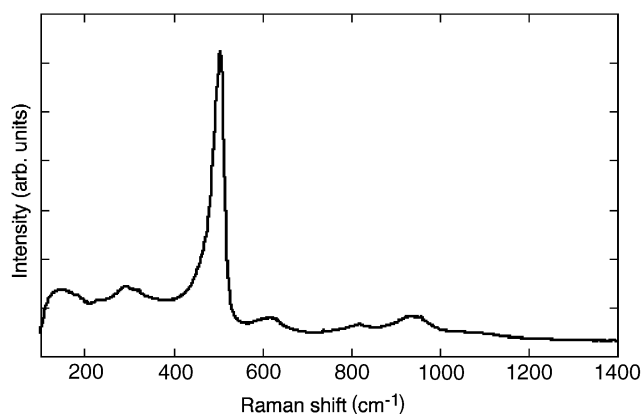


Fig. 5. Raman spectrum of a sample of LiSi synthesized at 2.5 GPa and 700°C. No Li<sub>12</sub>Si<sub>7</sub> was detected by X-ray diffraction, and there is no indication of Si impurity in the spectrum.

framework. Other new bands are present at lower frequency (324, 288, 226 and perhaps 160 cm<sup>-1</sup>): we can assign these to Si–Si–Si bending vibrations and to librational modes associated with the Li<sup>+</sup> ions.

<sup>29</sup>Si MAS NMR spectroscopy is an ideal technique for investigating details of local structure. The <sup>29</sup>Si MAS NMR spectrum of LiSi (Fig. 6) exhibits a peak at

–106.5 ppm (relative to tetramethylsilane, TMS: Si(CH<sub>3</sub>)<sub>4</sub>). The alkali monosilicides *MSi* (*M* = Li, Na, K, Rb, Cs) are generally remarkable in that they contain the unusual 3-coordinated Si<sup>-</sup> anion. This oxidation state and coordination geometry are highly unusual for Si, and it was interesting to establish the chemical shift systematics within the series (Fig. 7). The <sup>29</sup>Si MAS NMR spectrum of NaSi was reported recently elsewhere [14,15]. NaSi, KSi, RbSi and CsSi all contain two crystallographic silicon sites in their structures, so that two distinct <sup>29</sup>Si resonances are expected to occur. Both peaks were observed previously for NaSi [14,15], and for KSi and RbSi in this work: for CsSi, however, the peaks were unresolved (Fig. 7). Unlike LiSi, all of these compounds have structures based upon isolated Si<sub>4</sub><sup>4-</sup> tetrahedra [1] (Fig. 1).

The measured <sup>29</sup>Si chemical shifts within the *M* = Na, K, Rb, Cs alkali monosilicide series range from –280 to –360 ppm. These large values indicate strongly deshielded chemical environments for the Si nucleus [14]. Among covalent tetrahedrally coordinated silicon compounds with formal oxidation state zero, TMS (Si(CH<sub>3</sub>)<sub>4</sub>) is the reference compound with  $\delta_{\text{Si}} = 0$ , elemental semiconducting Si occurs at –76.5 ppm, SiH<sub>4</sub> at –95 ppm, and Si(Si(CH<sub>3</sub>)<sub>3</sub>)<sub>4</sub> at –138 ppm [16]. The correlations here reflect the relative electronegativity at the Si site, and the degree of *s* orbital participation in the bonding. Covalently bonded, tetrahedrally coordinated neutral silicon has its *s*, *p* bonding states completely filled within *sp*<sup>3</sup> hybridization. Formation of Si<sup>-</sup> in the silicides results in a lone pair occupying one of the *sp*<sup>3</sup> hybrid lobes, resulting in a ~100 ppm shift of <sup>29</sup>Si NMR signals to more deshielded values. We have

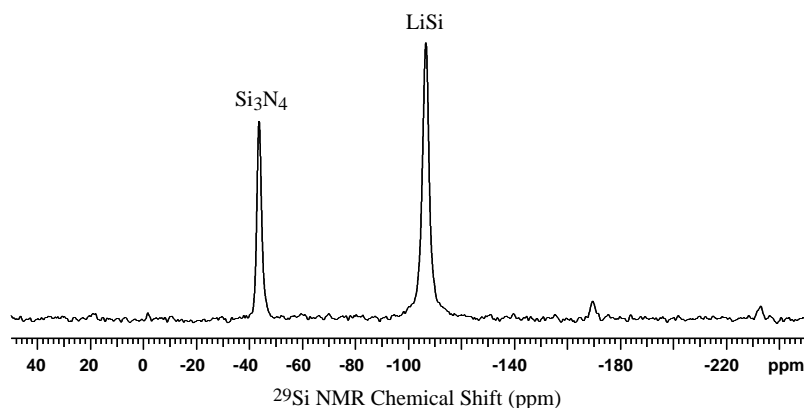


Fig. 6. MAS NMR  $^{29}\text{Si}$  spectrum of LiSi (8 kHz spinning speed), referenced to tetramethylsilane (TMS). The peak at  $-45.5$  ppm is due to the  $\text{Si}_3\text{N}_4$  rotor, and that at  $-106.5$  ppm is due to the unique crystallographic Si site in LiSi. The weak peaks near  $-170$  and  $-232$  ppm are due to  $\text{Si}_3\text{N}_4$  spinning side bands.

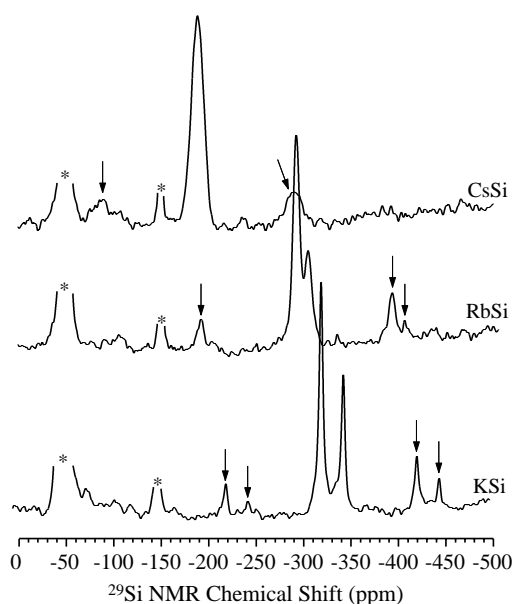


Fig. 7.  $^{29}\text{Si}$  MAS NMR spectra of CsSi, RbSi and KSi. The  $^{29}\text{Si}$  resonance from the  $\text{Si}_3\text{N}_4$  rotor and its side bands are marked by asterisks. The main resonances for the alkali monosilicides consist of two peaks for RbSi and KSi, and a single unresolved broad band for CsSi. The spinning side bands associated with these bands are indicated by arrows. The relative intensities for the two peaks for RbSi and KSi (including the side band intensities) occur in an approximately 3:1 intensity ratio. This allows the peaks to be assigned to the  $24f$  and  $8e$  crystallographic sites, respectively.

plotted the  $^{29}\text{Si}$  NMR shifts among the alkali silicide series as a function of the metal ionization energy (Fig. 8). There is a regular trend to more negative shifts from Cs to Na, within the isostructural ( $\text{Si}_4^{4-}$  tetrahedra) series, that is consistent with the expected degree of electron transfer from the metal atom. The chemical shift for LiSi is considerably less deshielded than expected ( $\delta(^{29}\text{Si}) \sim -100$  ppm, compared with a  $-400$  ppm value that was predicted from the “chemical” trend shown in Fig. 8), thus placing LiSi more within the

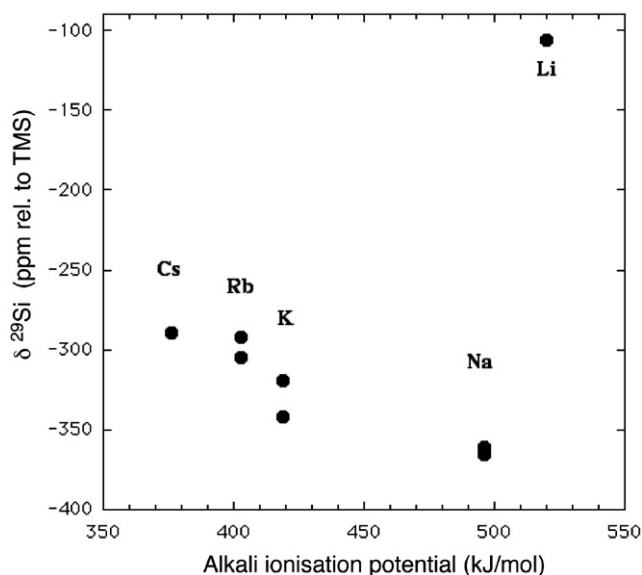


Fig. 8. Plot of  $^{29}\text{Si}$  chemical shifts in the alkali monosilicide series as a function of alkali atom ionization potential. (b)  $^7\text{Li}$  MAS NMR spectrum of LiSi, referenced to  $\text{Li}^+$  (aq). The central line has a quadrupolar line shape ( $I = 3/2$ ). The isotropic shift and quadrupolar parameters were estimated by fitting the spectrum (see text). The weak peaks symmetrically placed about the central band are spinning side bands.

range observed for covalent (Si, C, H) compounds [16]. This deviation could indicate a greater degree of covalency in Li–Si bonding compared with the other alkali metals, and it could be associated with the higher degree of connectivity observed within the  $\text{Si}^-$  framework of LiSi.

We also measured the  $^7\text{Li}$  MAS NMR spectrum for LiSi (Fig. 9). The spectrum exhibits a sharp central line with its maximum at  $11.3$  ppm (relative to  $\text{Li}^+$  in aqueous  $1$  M LiCl solution). From the positions of the spinning side bands and by fitting the quadrupolar lineshape, we estimated the position of the isotropic shift ( $\delta_{\text{iso}}$ ) as

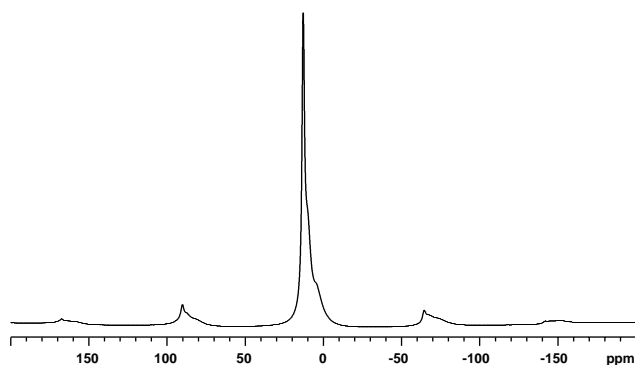


Fig. 9.  ${}^7\text{LiSi}$  MAS-NMR spectrum of LiSi.

12.6 ppm, and the quadrupolar parameters as  $\nu_Q = 281.6$  MHz,  $\eta = 0.9$  [16]. The small deviation of the  $\text{Li}^+$  electric field gradient from cylindrical geometry ( $\eta = 1$ ) is consistent with the crystalline environment: each Li atom has 6 Si neighbours between 2.6 and 3.1 Å, forming a roughly prismatic arrangement, along with 6 Li neighbours between 2.7 and 3.1 Å alternating with Si in the coordination environment [4]. The large value of the quadrupolar coupling constant ( $\nu_Q$ ) is indicative of asymmetry in the charge distribution at the  $\text{Li}^+$  sites. The partially covalent Li–Si bonds ( $\text{Li}^+ \cdots \text{Si}^-$ ) on one “side” of the Li coordination “cylinder” lie at 2.6–2.7 Å, and those on the other side occur between 2.7 and 3.1 Å. The fact that such a quadrupolar pattern is observed in the NMR lineshape indicates that the  $\text{Li}^+$  ions are “static” in the LiSi structure at ambient  $T$ . This is borne out by the small thermal parameters obtained from the Rietveld refinement (Table 1). Our study also gave preliminary information on the  ${}^7\text{Li}$  NMR spectrum of  $\text{Li}_{12}\text{Si}_7$ . In one run on a sample containing 3–4%  $\text{Li}_{12}\text{Si}_7$ , we observed an additional weak  ${}^7\text{Li}$  resonance at  $-15.6$  ppm that was flanked by spinning side bands at 48.6 and  $-79.9$  ppm (relative to  $\text{Li}^+$  (aq)). We assign these features to the impurity  $\text{Li}_{12}\text{Si}_7$  phase. The central peak was more symmetric than that for LiSi, and was much sharper, indicating that  $\nu_Q$  for  ${}^7\text{Li}$  in  $\text{Li}_{12}\text{Si}_7$  is smaller than for LiSi.

The DC electrical conductivity of cold-pressed LiSi pellets synthesized by the piston-cylinder technique was measured as a function of temperature between 250 and 650 K (Fig. 10). The conductivity increases with increasing temperature, indicating semiconducting behaviour with a narrow band gap  $E_b = 0.057$  eV, for  $T < 450$  K. The gap is smaller than that recorded for the black form of phosphorus,  $E_b = 0.33$  eV [17], that is isolectronic and isostructural with the  $\text{Si}^-$  framework in LiSi. It is obvious that donation of electrons from Li into the conduction band of the Si framework occurs in LiSi. There is an unexpected rapid increase in DC conductivity of LiSi between 450 and 525 K. This behaviour contrasts with that of  $\text{Li}_{12}\text{Si}_7$ , which shows an increase in its conductivity with temperature below 230 K, and a

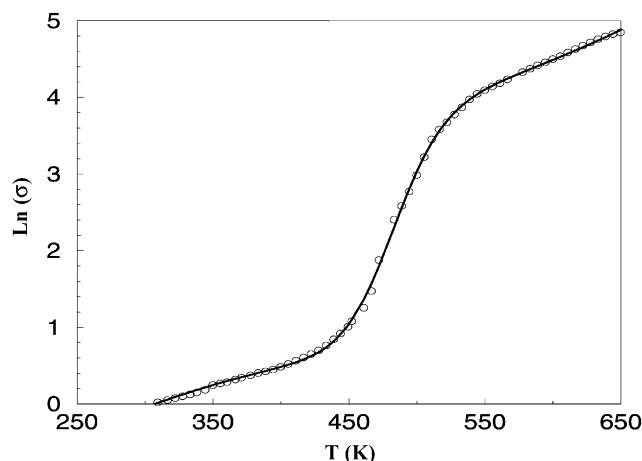


Fig. 10. DC electrical conductivity as a function of temperature for a pressed disc of LiSi sample.

sharp decrease in conductivity above this temperature [18].  $\text{Li}_{12}\text{Si}_7$  has a structure containing pentagonal  $\text{Si}^-$  rings and 4-membered planar “stars”: it has been proposed that the decreased conductivity observed at high temperature for this compound is due to creation of  $\text{Li}^+$  vacancies [18,19]. In the case of LiSi, the increased conductivity as a function of temperature could also indicate the onset of a  $\text{Li}^+$  contribution to the conduction mechanism.

#### 4. Conclusion

In summary, the formation of LiSi could be achieved in good yield at pressures of 1–2.5 GPa, at temperatures between 500°C and 700°C, providing large amounts of the new material with its unusual Si–Si bonding geometry for further studies. The samples prepared here were characterized by  ${}^{29}\text{Si}$  and  ${}^7\text{Li}$  MAS NMR spectroscopy and Raman scattering.  ${}^{29}\text{Si}$  NMR results within the  $M\text{Si}$  alkali monosilicide series ( $M = \text{Na}, \text{K}, \text{Rb}, \text{Cs}$ ) are consistent with increased electron transfer to the  $\text{Si}^-$  polyanion from the more electropositive metals. LiSi falls off the trend, indicating increased covalency of the Li–Si bond. Electrical conductivity measurements indicate that LiSi is a narrow gap electronic semiconductor at room temperature, with  $\text{Li}^+$  ions fixed on crystallographic sites within the structure. A large increase in conductivity above 450 K indicates the possible onset of  $\text{Li}^+$  mobility at high temperature.

#### Acknowledgments

The initial studies were supported by the NSF MRSEC program, and by the NSF-funded REU program through grants to PFM and JG. PFM and

JG also acknowledge “start-up” support from Jacksonville State University, Alabama, University College London and the Royal Institution. The authors thank K. Leinenweber for assistance with high-pressure synthesis experiments, and M. Williams and E. Soignard for NMR and Raman spectroscopy (NMR instrumentation supported by NSF grant CHE-9808678). We also acknowledge discussions with J. Dong, A. Chizmeshya, and J. Hernlund. PFM is a Wolfson-Royal Society Research Merit Award holder.

## References

- [1] M. Kauzlarich, *Chemistry, Structure, and Bonding of Zintl Phases and Ions*, VCH, New York, 1996.
- [2] H. Schäfer, *Ann. Rev. Mater. Sci.* 15 (1985) 1.
- [3] R. Nesper, *Prog. Solid State Chem.* 20 (1990) 1.
- [4] J. Evers, G. Oehlinger, G. Sextl, *Angew. Chem. Int. Ed. Engl.* 32 (1993) 1442.
- [5] J. Evers, G. Oehlinger, G. Sextl, *Eur. J. Solid State Inorg. Chem.* 34 (1997) 773.
- [6] C. Vandermarel, G.J.B. Vinke, W. Vanderlugt, *Solid State Commun.* 54 (1985) 917.
- [7] A. Brown, S. Rundqvist, *Acta Cryst.* 19 (1965) 684.
- [8] E. Menges, V. Hopf, H. Schäfer, A. Weiß, *Z. Naturforsch. B* 24 (1969) 1351.
- [9] C. Cros, M. Pouchard, P. Hagenmuller, *J. Solid State Chem.* 2 (1970) 570.
- [10] E. Reny, P. Gravereau, C. Cros, M. Pouchard, *J. Mater. Chem.* 8 (1998) 2839.
- [11] G.K. Ramachandran, J.-J. Dong, J. Diefenbacher, J. Gryko, R.F. Marzke, O.F. Sankey, P.F. McMillan, *J. Solid State Chem.* 145 (1999) 716.
- [12] J. Gryko, P.F. McMillan, R.F. Marzke, G.K. Ramachandran, D. Patton, S.K. Deb, O.F. Sankey, *Phys. Rev. B* 62 (2000) 7707.
- [13] A.C. Larson, R.B. Von Dreele, Los Alamos National Laboratory Technical Report LA-UR-86-748, 1987.
- [14] D. Mayeri, B.L. Phillips, M.P. Augustine, S.M. Kauzlarich, *Chem. Mater.* 13 (2001) 765.
- [15] J. He, D.D. Klug, K. Uehara, K.F. Preston, C.I. Ratcliffe, J.S. Tse, *J. Phys. Chem. B* 105 (2001) 3475.
- [16] G. Engelhardt, D. Michel, *High-Resolution Solid-State NMR of Silicates and Zeolites*, Wiley, New York, 1987.
- [17] R.W. Keyes, *Phys. Rev.* 92 (1953) 580.
- [18] K. Kuriyama, T. Maeda, A. Mizuno, *Phys. Rev. B* 38 (1988) 13436.
- [19] M.C. Bohm, R. Ramirez, R. Nesper, H.G. von Schnering, *Phys. Rev. B* 30 (1984) 4870.